Title

Physics-Conditioned Generative Adversarial Networks for State Estimation in Active Power Distribution Systems with Low Observability

Authors

Kamal, Mohasinina
Li, Wenting
Deka, Deepjyoti
et al.

Publication Date

2022-05-31

Peer reviewed

Physics-Conditioned Generative Adversarial Networks for State Estimation in Active Power Distribution Systems with Low Observability

Mohasinina Kamal, *Student Member, IEEE*, Wenting Li, *Member, IEEE*,
Deepjyoti Deka, *Senior Member, IEEE*, and Hamed Mohsenian-Rad, *Fellow, IEEE*

***Abstract*— A novel method is proposed to address the issue of low-observability in Distribution System State Estimation (DSSE). We first use the historical data at the unobservable locations to construct and train proper Generative Adversarial Network (GAN) models to compensate for lack of direct real-time measurements. We then integrate the trained GAN models, together with the direct synchronized measurements at the observable locations, into the formulation of the DSSE problem. In this regard, we simultaneously take advantage of the forecasting capabilities of the GAN models, the available real-time synchronized measurements, and the DSSE formulations based on physical laws in the power system. As a result, on one hand we conduct a *physics-conditioned* estimation of the unknown power injections at the unobservable locations; and on the other hand, we also achieve a complete DSSE solution for the understudy low-observable active power distribution system.**

***Keywords*: Distribution system state estimation, low-observability, physics-conditioned generative adversarial networks, distribution synchrophasors, active power distribution systems, power injection.**

I. Introduction

A. Background and Motivation

In Distribution System State Estimation (DSSE), the performance is directly affected by the availability of measurements and the extent of observability in the power distribution system, which depends on the type, number, and location of sensors [1]. In practice, power distribution feeders often suffer from *low observability*; because the number of sensors is often less than the number of state variables. The installation of smart meters in recent years has improved observability. However, their low reporting rates are not sufficient to capture the high dynamics of power distribution systems, which are caused by the growing penetration of distributed energy resources (DERs), the emergence of new types of loads such as electric vehicles, and the development of demand response programs [2].

Instead, we need to rely on the measurements which have much higher reporting rates, such as distribution-level phasor measurement units (D-PMUs) or micro-PMUs [3]. However, D-PMUs are expensive and require a proper communication infrastructure to collect the measurements. In this regard, the power distribution network still remains under low-observability conditions due to the use of only a few D-PMUs at each feeder.

Of course, lack of access to the measurements at behind-the-meter DERs is another factor that further contributes to the low-observability circumstances. This is due to reasons such as privacy regulations and/or the lack of proper communication infrastructure to support the utility's access to the behind-the-meter DERs in active power distribution systems.

The common approach to tackle low-observability in DSSE is to use pseudo-measurements. Pseudo-measurements are often constructed by using historical data, such as from smart meters [4]. However, it is often reported that pseudo-measurements are not accurate to properly address low-observability in DSSE problems. Inaccurate pseudo-measurements can create ill-conditioned mathematical optimization in the DSSE problem formulation; which may prevent it from converging to a reliable solution [5].

B. New Approach and Contributions

In this paper, we address the issue of low-observability in DSSE problems by taking a different approach. Our new approach is motivated by the fact that, in practice, while it is *not* possible to have direct real-time access to high-resolution measurements at a subset of the buses in the power distribution system, it often *is* doable to have access to the *historical data* or the probability distribution of such data at the unobservable buses. Hence, we propose to start from the available historical data but through an innovative process we turn them into something close to what we could obtain through direct real-time measurements at these unobservable locations.

We first use the historical data at the unobservable locations to construct and train proper Generative Adversarial Network (GAN) models to compensate for lack of direct real-time measurements. We then integrate the trained GAN models, together with the direct real-time synchronized measurements at the observable locations, into the formulation of the DSSE problem. Thus, we simultaneously take advantage of the forecasting capabilities of the GAN models, the available real-time synchronized measurements, and the DSSE formulations based on *physical laws* in the power system in the power flow equations.

In this regard, our contributions are two-fold. On one hand we conduct a physics-conditioned estimation of the unknown power injections at the unobservable locations, i.e., at the buses where direct measurements are not available. On the other hand, we ultimately achieve a complete DSSE solution for the understudy low-observable active power distribution system.

M. Kamal and H. Mohsenian-Rad are with the University of California, Riverside, CA, USA. W. Li and D. Deka are with Los Alamos National Laboratory, Santa Fe, NM, USA. The corresponding authors are H. Mohsenian-Rad and D. Deka. E-mails: hamed@ece.ucr.edu, deepjyoti@lanl.gov. This work is supported in part by a Summer Internship at the Center for Nonlinear Studies (CNLS) at LANL, UCOP grant LFR-18-548175, and the LDRD program of Los Alamos National Laboratory under project number 20210078DR.

C. Literature Review

In [6], a Gaussian mixture model is used to enhance the statistical modeling of the pseudo-measurements in state estimation for inclusion in a conventional weighted least square (WLS)-DSSE. In [7], a two-stage data clustering method is used to construct the pseudo-measurements. In [8], artificial neural networks are trained to generate pseudo-measurements from limited measurements. In [9], a deep neural network is trained to estimate the state variables with limited observations.

While the above methods make pseudo-measurements more robust against system uncertainties, they process the pseudo-measurements as is, i.e., they do *not* condition the characteristics of the pseudo-measurements to the physics of the underlying power circuit. Conducting physics-conditioned analysis of the historical data is the main focus in this paper.

In this regard, our work is more related to the studies such as in [10], where a new data-driven method is proposed based on training a deep neural network model to solve the DSSE problem by adding physical information of the underlying power distribution feeder, such as the parameters of the distribution lines to further increase the accuracy. Our approach, on the other hand, optimizes the output of a GAN model to estimate the unknown power injection at unobservable loads by utilizing the available measurements in physical equations. The results are then used in order to solve the DSSE problem.

Low-observability in the DSSE problem can be addressed also by using concepts from sparse recovery, e.g., see [11], [12]. While we do not consider the analysis of sparsity in this paper, our approach can be extended in the future to include sparse recovery *together with* the physics-conditioned GAN models.

The rest of this paper is organized as follows. In Section II, a full description of the system model is presented. Section III covers the overall methodology in three stages to reach to the final DSSE results. The case studies are analyzed in Section IV. The conclusions are discussed in Section V.

II. System Model

Our system model is based on the popular DistFlow equations with N buses [13], [14]. Accordingly, we define the state variables in a power distribution system based on two vectors:

$$\mathbf{y} = \left[\begin{array}{cccc} y_1 & y_2 & \dots & y_N \end{array} \right]^T, \tag{1}$$

$$\boldsymbol{\delta} = \left[\begin{array}{cccc} \delta_1 & \delta_2 & \dots & \delta_N \end{array} \right]^T, \tag{2}$$

where $\mathbf{y}$ denotes the vector of the *square of the magnitude* of the voltage phasors at all buses, and δ denotes the vector of the *phase angle* of the voltage phasors at all buses.

A. Grouping of Buses

We divide the buses in the power distribution feeder into three categories based on the type of available data:

- **Group 1**: The buses where we have access to voltage phasor measurements and power injections by using D-PMUs.
- **Group 2**: The buses where we do *not* have access to voltage phasor measurements, because these buses are not equipped with D-PMUs, but we *do* have access to the power injection measurements at regular meters or at the DERs.
- **Group 3**: The buses where we have no access to any type of direct measurements. These are the *unobservable* buses in the system. At these buses, we rather only have access to the *historical data* for the unknown power injections.

As we will show in Section II-B, the following relationship holds across the measurements in these three groups of buses:

$$\left[\begin{array}{c} \Delta\mathbf{y}^m \\ \Delta\boldsymbol{\delta}^m \end{array} \right] = \mathbf{Z^m} \left(\mathbf{S}^m + \mathbf{S}^n \right), \tag{3}$$

where superscript m indicates direct measurements and superscript n indicates *lack* of direct measurements. Here, $\Delta\mathbf{y}^m$ is the vector that is constructed based on the differences between the entries in vector $\mathbf{y}$ at two buses that belong to Group 1, where the phasor measurements are directly measured. Similarly, $\Delta\boldsymbol{\delta}^m$ is the vector that is constructed based on the differences between the entries in vector $\boldsymbol{\delta}$ at two buses that belong to Group 1. Vector $\mathbf{S}^m$ is a properly defined vector of the power injections at the buses that belong to Group 1 or Group 2. The power injections in this vector *are* measured. Vector $\mathbf{S}^n$ is a properly defined vector of the power injections at the buses that belong to Group 3. The power injections in this vector are *not* measured; thus they are not known. Matrix $\mathbf{Z^m}$ is a modified version of a properly defined impedance matrix $\mathbf{Z}$ to relate the power injections to the available phasor measurements.

From (3), we can relate the *known* voltage phasor measurements in Group 1 on the left-hand-side, to the *known* power injection measurements in Groups 1 and 2 as well the *unknown* power injections in Group 3 on the right-hand-side. Note that, the unknown voltage phasors at the unobservable buses are intentionally left out of the formulation in (3). We will use the expression in (3) to develop our methodology in Section III.

B. Deriving the Circuit Equations

In this section, we explain how to derive the expression in (3). Our analysis here is inspired by the formulations in [14]. From the linearized DistFlow equations we have [13]:

$$y_i - y_j \approx r_{i,j} P_{i,j} + x_{i,j} Q_{i,j}, \tag{4a}$$

$$\delta_i - \delta_j \approx x_{i,j} P_{i,j} - r_{i,j} Q_{i,j}, \tag{4b}$$

where $r_{i,j}$ and $x_{i,j}$ denote the resistance and reactance of the line segment between nodes i and j, respectively; and $P_{i,j}$ and $Q_{i,j}$ denote the active power and the reactive power flowing on the line that goes from node i to node j, respectively.

1) Line Topology: In a feeder with a line topology, such as the one shown in Fig. 1(a), we have:

$$P_{i,j} = \sum_{k=j}^{N} p_k, \quad Q_{i,j} = \sum_{k=j}^{N} q_k, \tag{5}$$

where p_k and q_k are the net active power consumption and the net reactive power consumption at bus k, respectively. Since the network has a line topology, the nodes are denoted from 1 to N and they are all located one after another across a line.

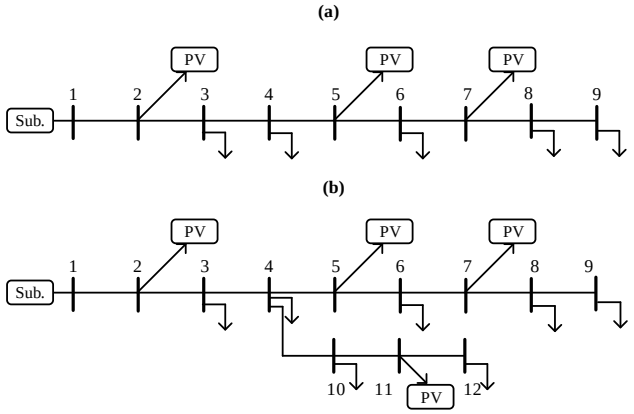

Fig. 1: Two example power distribution network topologies: (a) a line topology with 9 buses; (b) a radial topology with 12 buses across a main and a lateral.

Suppose buses 1 and 3 belong to Group 1. They provide the following measurements: y_1^m, δ_1^m, y_3^m, δ_3^m. From (4), we have:

$$\begin{aligned}\Delta y_{1,3}^m &= y_1^m - y_3^m \\ &= (y_1 - y_2) + (y_2 - y_3) \\ &= (r_{1,2}P_{1,2} + x_{1,2}Q_{1,2}) + (r_{2,3}P_{2,3} + x_{2,3}Q_{2,3})\,. \end{aligned} \quad (6)$$

From (5), and after reordering the terms in (6), we obtain:

$$\Delta y_{1,3}^m = \begin{bmatrix} r_{1,2} \\ r_{1,2}+r_{2,3} \\ \vdots \\ r_{1,2}+r_{2,3} \\ x_{1,2} \\ x_{1,2}+x_{2,3} \\ \vdots \\ x_{1,2}+x_{2,3} \end{bmatrix}^T \begin{bmatrix} p_2 \\ p_3 \\ \vdots \\ p_9 \\ q_2 \\ q_3 \\ \vdots \\ q_9 \end{bmatrix}, \quad (7)$$

where the first vector in the right hand side constitutes the component of the modified impedance matrix $\mathbf{Z^m}$.

Next, suppose for the network in Fig. 1(a) we have:

$$\text{Group } 3 = \big\{2, 5, 7\big\},$$

which means that all the buses with PV units belong to the set of the unobservable buses in Group 3. Accordingly, we can decompose the second vector on the right-hand-side in (7) as a summation of two vectors: a vector in which we replace p_2, p_5, and p_7 with zero, and another vector in which we replace p_1, p_3, p_4, p_6, p_8, and p_9 with zero. The former will give us the corresponding components of $\mathbf{S}^m$, while the latter will give us the corresponding components of $\mathbf{S}^n$; see the expression in (3).

A similar expression can be obtained for $\Delta\delta_{1,3}^m = \delta_1^m - \delta_3^m$. By repeating this analysis for any two consecutive buses in Group 1, see [14], we can fully obtain the expression in (3).

2) Radial Topology with Laterals: Next, consider a radial feeder with a lateral, such as the one shown in Fig. 1(b). Since the lateral starts at bus 4, the formulation for $P_{1,2}$, $P_{2,3}$, and P_{34} remains the same as in (5). In fact, the formulation for $P_{10,11}$ and $P_{11,12}$ also remain the same as in (5). However, we need to update the formulations at the following six cases:

$$P_{4,5} = \sum_{k=5}^{9} p_k, \quad P_{5,6} = \sum_{k=6}^{9} p_k, \quad P_{6,7} = \sum_{k=7}^{9} p_k, \quad (8)$$

$$P_{7,8} = \sum_{k=8}^{9} p_k, \quad P_{8,9} = \sum_{k=9}^{9} p_k, \quad P_{4,10} = \sum_{k=10}^{12} p_k. \quad (9)$$

From the above, we can start from a formulation similar to the one in (6) and ultimately obtain a formulation similar to (7) which can lead to an expression as in (3) for a radial network.

In all cases, the left hand side in (3) would contain the state variables (square of the magnitude and phase angle) at the buses *with* D-PMUs; and the right hand side would contain a multiplication of a vector of resistances and reactances of the line segments and a vector of the net active and the net reactive power consummations at *all* the buses across the feeder.

C. Low-Observability Conditions

Let N_1, N_2, and N_3 denote the number of buses in Groups 1, 2, and 3, respectively. We have $N_1 + N_2 + N_3 = N$, where N is the total number of buses. Our focus in this paper is on the low-observability circumstances in power distribution feeders. In particular, we assume that the following inequality holds:

$$N_3 > N_1 - 1, \quad (10)$$

where the left-hand-side indicates the total number of unknowns in (3) while the right-hand-side indicates the total number of independent equations. To be exact, we shall express (10) as $2N_3 > 2(N_1 - 1)$ due to the analysis being in complex domain; however, once we divide both sides by two, we can reach (10).

Under the condition in (10), the system of linear equations in (3) is *under-determined*, i.e., it has an infinite number of solutions. This is because we have *more unknowns than independent equations*. As a result, one cannot solve the system of linear equations in (3) to estimate the unknown power injections at the buses in Group 3. Therefore, more efforts are needed to address low-observability, as we will explain in the next section.

III. Methodology

We develop our DSSE method in three stages:

- **Stage 1**: We use a GAN model to *learn* and *mimic* the characteristics of the power injections at the unobservable buses in Group 3 based on the available historical data.
- **Stage 2**: We replace the vector of unknown power injections $\mathbf{S}^n$ in (3) with the corresponding GAN models that we learned in the first stage. We then solve an optimization problem based on (3) to best estimate $\mathbf{S}^n$ in terms of the output of the GAN models as well as the direct measurements from Groups 1 and 2, while maintaining the physics-based relationships in (3). Here, the optimization variables are the input of the trained GAN model to provide us with a direct estimation for the unknown vector $\mathbf{S}^n$.
- **Stage 3**: Once we obtained $\mathbf{S}^n$ in the second stage, we use it together with the available measurements in $\mathbf{S}^m$ and the measurements in $\mathbf{y}^m$ and $\boldsymbol{\delta}^m$ to formulate and solve a

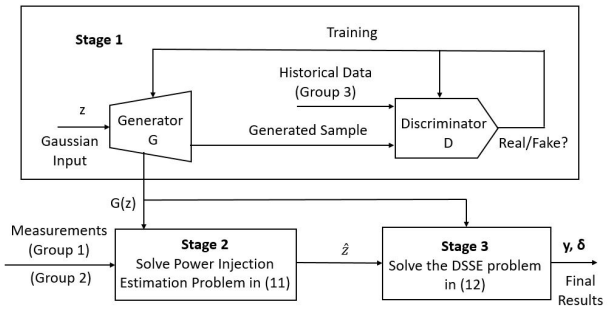

Fig. 2: The three stages in the proposed method and their interactions.

standard DSSE problem in order to estimate all the state variables in $\mathbf{y}$ and $\boldsymbol{\delta}$ across the power distribution system.

Next, we explain the details in each of the above stages. Without loss of generality, we assume that the buses in Group 3 always include all the solar power generation units.

A. Stage 1: Training the GAN Model

The layout of the internal components in Stage 1 in our proposed method is shown in the top box in Fig. 2. Here we train the two deep neural networks (DNNs) in the GAN model, namely the generator G and the discriminator D, to learn a probability distribution based on the historical data for power injection at buses in Group 3; and we accordingly generate new samples from the input noise z based on the probability distribution that we have learned in the GAN model. Importantly, the GAN model leverages the power of DNNs to express complex nonlinear relationships (at the generator) as well as to classify complex signals (at the discriminator), c.f. [15]. The outcome of the training process in Stage 1 is the generator model $G(z)$ for the power injections at the buses in Group 3.

Since we assume that Group 3 includes all the buses with solar power generation units, the GAN model here essentially learns the probability distribution for the output of the solar power generation units based on their historical data. For solar profile generation, Wasserstein GAN (WGAN) has been used in [16]. In our approach, we also use WGAN; because its training process is more stable and less sensitive to model architecture and choice of hyperparameter configurations [17].

B. Stage 2: Estimating the Unknown Solar Power Injections

Given the trained GAN model from Stage 1, we can now replace the unknown vector $\mathbf{S}^n$ in (3) with the vector of trained GAN models $\mathbf{G}(z)$. Of course, if we change z, then we obtain a different output from $\mathbf{G}(z)$; in other words, the GAN model still does not provide us with an actual vector $\mathbf{S}^n$, unless we also obtain the proper z to serve as the input to the GAN model.

We address this issue by formulating and solving a *physics-conditioned* optimization problem to find the optimal choice for z that can best capture the *physical relations* between the available direct measurements in Groups 1 and 2 with the power injections of the solar generation units in Group 3; while taking into consideration the fact that the probability distribution for such unknown power injections follow the trained GAN model.

In this regard, we formulate the following optimization problem to estimate the unknown solar power injections:

$$\underset{z}{\textbf{minimize}} \quad \left\| \begin{bmatrix} \Delta\mathbf{y}^m \\ \Delta\boldsymbol{\delta}^m \end{bmatrix} - \mathbf{Z}^{\mathbf{m}} \left(\mathbf{S}^m + \mathbf{G}(z)\right) \right\|_2^2. \tag{11}$$

Problem (11) can be solved by using the gradient descent method [18]. Since the generative model $\mathbf{G}(\cdot)$ is differentiable, we iteratively evaluate the gradient of the objective function in (11) with respect to z by using the backpropagation method, applying a second order diminishing step size at each iteration.

Once we obtain $\hat{z}$ as the solution, we can plug it in the *already trained* generator function of the GAN model, to obtain the estimated power injection profile as $\mathbf{G}(\hat{z})$ at the solar connected buses. Once this is done, the network becomes fully observable, where we know the power injection at each bus, either through direct measurements or as the estimated generation $\mathbf{G}(\hat{z})$.

We end this section with a clarifying note. Suppose instead of solving the problem in (10) as is over z, we attempt to solve it over $\mathbf{G}(z)$. In that case, this optimization would turn into a failed attempt to solve the under-determined system of equations in (3). However, by conducting the optimization over z, we take into account the distribution of the historical data that is learned by the GAN model to find the unknown power injections at the buses in Group 3 such that, they fit *not only* the system of equations in (3), *but also* the GAN model that we have trained by using the historical data. This novel approach resolves the initial under-determined nature of the system of equations in (3).

C. Stage 3: Obtaining the Final DSSE Results

The process in Stage 1 and Stage 2 makes the power distribution network fully observable. In other words, it eliminates Group 3 and essentially moves all the buses from Group 3 to Group 2. Therefore, what is left to do is to complete the DSSE task by solving the following optimization problem:

$$\underset{\mathbf{y},\boldsymbol{\delta}}{\textbf{minimize}} \quad \left\| \begin{bmatrix} \Delta\mathbf{y} \\ \Delta\boldsymbol{\delta} \\ \mathbf{y} \\ \boldsymbol{\delta} \end{bmatrix} - \begin{bmatrix} \mathbf{Z}\left(\mathbf{S}^m + \mathbf{G}(\hat{z})\right) \\ \mathbf{y^m} \\ \boldsymbol{\delta^m} \end{bmatrix} \right\|_2^2. \tag{12}$$

We may clarify a few notes about the above formulation. First, the solution of the optimization problem in (11) serves as a constant in the optimization problem in (12). In fact, the entire expression $\mathbf{Z}(\mathbf{S}^m + \mathbf{G}(\hat{z}))$ is a constant as far as solving the problem in (12) is concerned. Second, the impedance matrix $\mathbf{Z}$ in (12) is different from the impedance matrix $\mathbf{Z}^m$ in (11). While matrix $\mathbf{Z}^m$ relates the power injections across the feeder to the voltage phasor *measurements* at the buses in Group 1, matrix $\mathbf{Z}$ relates the power injections across the feeder to the voltage phasors at *all* the buses in the system. Third, the optimization variables in (12) include *all* the voltage phasors in the system, as represented by the square of their magnitude $\mathbf{y}$ and their phase angles $\boldsymbol{\delta}$. Fourth, the least square optimization problem in (12) includes the circuit equations on the top, which are expressed in terms of $\Delta\mathbf{y}$ and $\Delta\boldsymbol{\delta}$, as well as the direct measurements on the bottom, which are expressed in terms of $\mathbf{y}$ and $\boldsymbol{\delta}$ in comparison with $\mathbf{y}^m$ and $\boldsymbol{\delta}^m$, respectively. The former formulation is an

extension of the formulation in (3) to incorporate the voltage phasors at *all* buses. For example, while we defined $\Delta y^m_{1,3}$ as the first row in $\Delta \mathbf{y}^m$, here we define $\Delta y_{1,2}$ as the first row in $\Delta \mathbf{y}$. Finally, since the definition of synchrophasors requires a reference, we take the direct phasor measurements at bus 1 as the reference, i.e., the phase angles at all buses are calculated in reference to the phase angle at bus 1. This is a common approach in state estimation using synchronized phasor measurements [19].

IV. Case Studies

In this section, we present proof-of-concept case studies to demonstrate and to assess the performance of the proposed methods. For the cases where we examine the *line* topology in Fig. 1(a), we consider the following grouping of the buses:

$$\begin{aligned} &\text{Group } 1 = \{1, 9\}, \\ &\text{Group } 2 = \{3, 4, 6, 8\}, \\ &\text{Group } 3 = \{2, 5, 7\}. \end{aligned} \tag{13}$$

As for the cases where we examine the *radial* topology in Fig. 1(b), we consider the following grouping of the buses:

$$\begin{aligned} &\text{Group } 1 = \{1, 9, 12\}, \\ &\text{Group } 2 = \{3, 4, 6, 8, 10\}, \\ &\text{Group } 3 = \{2, 5, 7, 11\}. \end{aligned} \tag{14}$$

Notice that the condition in (10) holds for both (13) and (14).

For the purpose of comparison, we generated 100 different scenarios with different solar generation profiles and different background loads, including variable loads at buses 4 and 6 at both topologies at each scenario. Our goal here is to look at the overall improvement statistics rather than a single scenario.

For training and simulation we use the synthetic solar photovoltaic (PV) power plant data from the NREL open-source resources [20]. The implementation of the GAN model is programmed by standard open source platforms, see [21].

A. Performance Measures

Given that the proposed methodology has multiple stages, we use two metrics to evaluate the performance:

- First, we assess the accuracy of the proposed method in estimating the unknown power injections at the PV units in each scenario. This would be the output of the physics-conditioned optimization in (11). To obtain this measure, we compare the *mean square error* (MSE) for the daily profiles of the estimated solar generations with the real solar measurements of the 100 scenarios. We do this for both the estimated $\mathbf{G}(\hat{z})$ and for the ordinary GAN output $\mathbf{G}(z)$ with a random z, to see how much of an improvement we can get by adding physics-conditioned optimization.
- Second, we assess the accuracy of the ultimate state estimation results, i.e., the accuracy of the output of the optimization problem in (12). In this regard, we define *mean absolute error* (MAE) in form of the standard *total vector error* (TVE) analysis in the field of phasor measurements:

$$\text{MAE} = \textbf{Mean}\left\{\frac{|\sqrt{\hat{\mathbf{y}}}\angle\hat{\boldsymbol{\delta}} - \sqrt{\mathbf{y}}\angle\boldsymbol{\delta}|}{|\sqrt{\mathbf{y}}\angle\boldsymbol{\delta}|}\right\} \times 100\%, \tag{15}$$

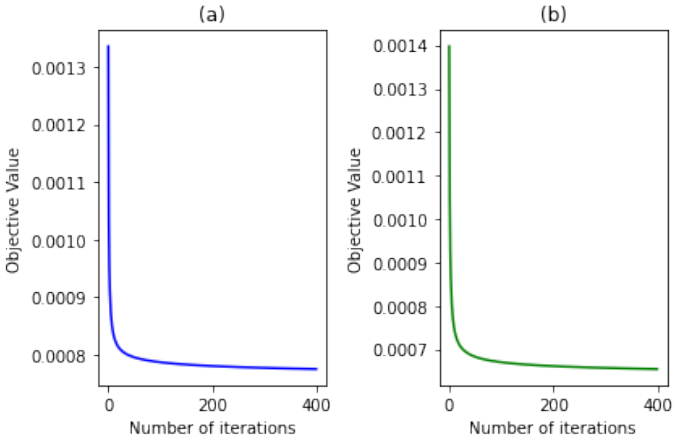

Fig. 3: Analysis of convergence: the objective value versus the iteration number in solving problem (11) for: (a) line topology; (b) radial topology.

where $\hat{\mathbf{y}}\angle\hat{\boldsymbol{\delta}}$ is the estimated voltage phasor that is obtained by solving the DSSE optimization problem in (12). Here the *mean* is calculated across all the buses in the system.

B. Convergence

An important property in solving the problem in (11) is the ability for the gradient iterations to converge. This property is investigated in Figs. 3(a) and (b), for the line topology and the radial topology, respectively. In both cases, convergence is achieve within 400 iterations. Here we have used a second order diminishing step size which removes fluctuations in the objective value and helps reach convergence faster.

C. Performance in Estimating Unknown Power Injections

Next, we compare the results after convergence with the case of the ordinary GAN training, i.e., the case where we do *not* apply physics-conditioning to the output of the GAN model. The results are shown in Figs. 4(a) and (b) for the line topology and the radial topology, respectively. In both cases, the proposed method has much lower MSE values compared to the one without physics-conditioning. Overall, on average, our method can reach up to $28\% \sim 29\%$ less pseudo-measurement error compared to the ordinary GAN. These results are very promising and confirm the effectiveness of combining the physics-conditioned GAN model formulation in the optimization problem in (11).

D. Performance in State Estimation

Finally, we evaluate the performance of the proposed method in achieving its ultimate goal, i.e., to enhance the accuracy in the DSSE problem. In this regard, we calculate and compare the MAE as defined in (15) for the case of using an ordinary GAN versus our proposed physics-conditioned GAN. Figs. 5 (a) and (b) show the improvements in the final DSSE outcome in a line topology and in a radial topology, respectively. In this experiment, we found our method to reduce the MAE on average by up to $29\% \sim 36\%$, over using the ordinary GAN model.

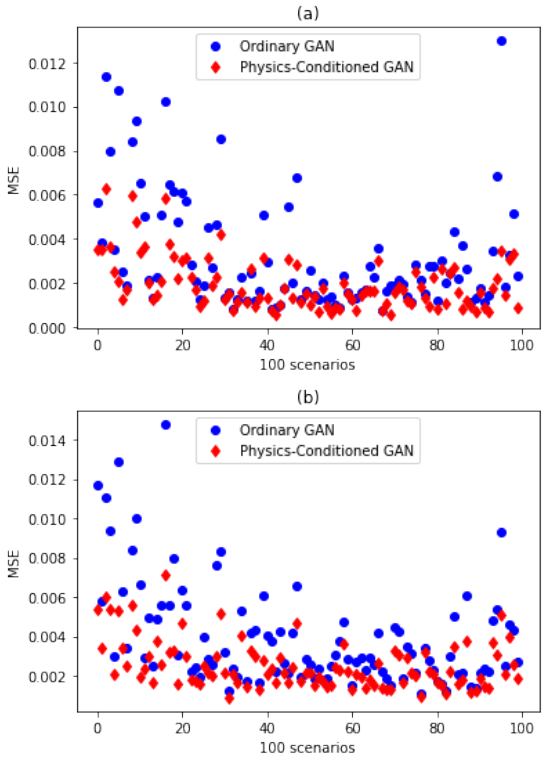

Fig. 4: Comparing the proposed method with the ordinary GAN in estimating the unknown power injections: (a) line topology; (b) radial topology.

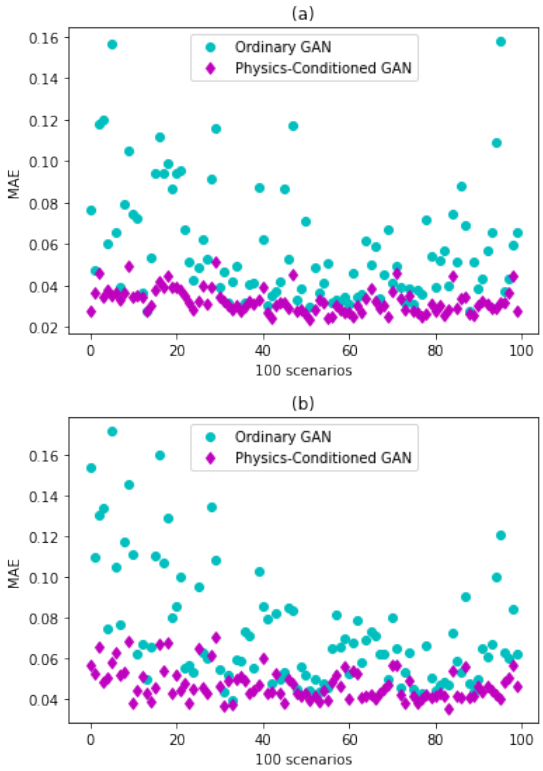

Fig. 5: Comparing the proposed method with the ordinary GAN in terms of the ultimate DSSE results: (a) line topology; (b) radial topology.

V. Conclusions

In this work, we showed that we can significantly improve the outcome of the GAN model training and the DSSE optimization in low-observable active power distribution networks by integrating them into proper physics-conditioned formulations with respect to the power flow equations. Accordingly, we can enhance the solution of the DSSE problem under low-observability conditions by enhancing our estimation of the power injections at unobservable buses, with assistance from the limited availability of the direct synchronized real-time measurements. On average, our method can reduce the error in pseudo-measurements by $28\% \sim 29\%$; and the ultimate error in state estimation by $29\% \sim 36\%$, over the case without physics-based conditioning of the trained GAN models.

References

[1] A. Abur and A. G. Exposito, *Power system state estimation: theory and implementation*. CRC press, 2004.

[2] A. S. Zamzam, X. Fu, and N. D. Sidiropoulos, "Data-driven learning-based optimization for distribution system state estimation," *IEEE Transactions on Power Systems*, vol. 34, no. 6, pp. 4796–4805, 2019.

[3] H. Mohsenian-Rad, E. Stewart, and E. Cortez, "Distribution synchrophasors: Pairing big data with analytics to create actionable information," *IEEE Power and Energy Magazine*, vol. 16, no. 3, pp. 26–34, May 2018.

[4] S. Bhela, V. Kekatos, and S. Veeramachaneni, "Enhancing observability in distribution grids using smart meter data," *IEEE Transactions on Smart Grid*, vol. 9, no. 6, pp. 5953–5961, 2017.

[5] K. A. Clements, "The impact of pseudo-measurements on state estimator accuracy," in *Proc. of the IEEE PES General Meeting*, Detroit, MI, 2011.

[6] R. Singh, B. Pal, and R. Jabr, "Distribution system state estimation through gaussian mixture model of the load as pseudo-measurement," *IET generation, transmission & distribution*, vol. 4, no. 1, pp. 50–59, 2009.

[7] Y. R. Gahrooei, A. Khodabakhshian, and R.-A. Hooshmand, "A new pseudo load profile determination approach in low voltage distribution networks," *IEEE Transactions on Power Systems*, vol. 33, no. 1, pp. 463–472, 2017.

[8] E. Manitsas, R. Singh, B. C. Pal, and G. Strbac, "Distribution system state estimation using an artificial neural network approach for pseudo measurement modeling," *IEEE Transactions on Power Systems*, vol. 27, no. 4, pp. 1888–1896, 2012.

[9] K. R. Mestav, J. Luengo-Rozas, and L. Tong, "Bayesian state estimation for unobservable distribution systems via deep learning," *IEEE Transactions on Power Systems*, vol. 34, no. 6, pp. 4910–4920, 2019.

[10] J. Ostrometzky, K. Berestizshevsky, A. Bernstein, and G. Zussman, "Physics-informed deep neural network method for limited observability state estimation," *arXiv preprint arXiv:1910.06401*, 2019.

[11] S. S. Alam, B. Natarajan, and A. Pahwa, "Distribution grid state estimation from compressed measurements," *IEEE Transactions on Smart Grid*, vol. 5, no. 4, pp. 1631–1642, 2014.

[12] A. Akrami, S. Asif, and H. Mohsenian-Rad, "Sparse tracking state estimation for low-observable power distribution systems using D-PMUs," *IEEE Transactions on Power Systems, accepted*, July 2021.

[13] M. E. Baran and F. F. Wu, "Optimal capacitor placement on radial distribution systems," *IEEE Transactions on power Delivery*, vol. 4, no. 1, pp. 725–734, 1989.

[14] R. Dobbe, D. Arnold, S. Liu, D. Callaway, and C. Tomlin, "Real-time distribution grid state estimation with limited sensors and load forecasting," in *2016 ACM/IEEE 7th International Conference on Cyber-Physical Systems (ICCPS)*. IEEE, 2016, pp. 1–10.

[15] I. Goodfellow, J. Pouget-Abadie, M. Mirza, B. Xu, D. Warde-Farley, S. Ozair, A. Courville, and Y. Bengio, "Generative adversarial nets," *Advances in neural information processing systems*, vol. 27, 2014.

[16] Y. Chen, Y. Wang, D. Kirschen, and B. Zhang, "Model-free renewable scenario generation using generative adversarial networks," *IEEE Transactions on Power Systems*, vol. 33, no. 3, pp. 3265–3275, 2018.

[17] M. Arjovsky, S. Chintala, and L. Bottou, "Wasserstein generative adversarial networks," in *International conference on machine learning*, 2017.

[18] A. Bora, A. Jalal, E. Price, and A. G. Dimakis, "Compressed sensing using generative models," in *Int. Conference on Machine Learning*, 2017.

[19] H. Mohsenian-Rad, *Smart Grid Sensors: Principles and Applications*. Cambridge University Press, 2022.

[20] https://www.nrel.gov/grid/solar-power-data.html.

[21] A. Paszke, S. Gross, F. Massa, A. Lerer, J. Bradbury, G. Chanan, T. Killeen, Z. Lin, N. Gimelshein, L. Antiga, *et al.*, "Pytorch: An imperative style, high-performance deep learning library," *Advances in neural information processing systems*, vol. 32, pp. 8026–8037, 2019.